

# $W_e=100\text{nm}$ InP/InGaAs DHBT with Self-aligned MOCVD Regrown p-GaAs Extrinsic Base Exhibiting $1\Omega\text{-}\mu\text{m}^2$ Base Contact Resistivity

Yihao Fang, Hsin-Ying Tseng, and Mark J.W. Rodwell  
ECE, University of California Santa Barbara, Santa Barbara, CA, 93106, USA  
Email: [yihao.fang@ece.ucsb.edu](mailto:yihao.fang@ece.ucsb.edu) Phone: (424) 208-9822

We report DC results from a  $W_e=100\text{nm}$  InP/InGaAs DHBT technology with a self-aligned MOCVD regrown GaAs extrinsic base providing low base access resistance  $R_{bb}$  while maintaining acceptable DC current gain  $\beta$ . A  $0.09\times 5\mu\text{m}^2$  transistor exhibits a base contact resistivity  $\rho_c=1\Omega\text{-}\mu\text{m}^2$ , and a peak  $\beta\sim 15$ . The HBTs exhibit a common-emitter breakdown voltage  $BV_{CEO}=3.6\text{V}$  ( $J_C=10\mu\text{A}/\mu\text{m}^2$ ). According to the general scaling law for InP HBTs in [1], the low  $\rho_c$  meets the requirement for  $f_{max}=2.8\text{THz}$  operation.

InP/InGaAs DHBTs with  $f_{max}>1\text{THz}$  have been reported. The InGaAs bases in [2-3] are thinned to  $<25\text{nm}$  with a high carbon doping ( $>5\times 10^{19}\text{cm}^{-3}$ ) to achieve fast electron transport while supporting a low  $\rho_c$ . Further scaling to thinner base layer and higher doping concentration poses two major challenges: (1) the  $>4\text{nm}$  metal/semiconductor reaction depth of Pd- or Pt-based metal contacts diminishes transistor reliability [2], and (2) higher doping reduces the Auger-limited  $\beta$ , degrading the transistor noise figure NF. Therefore, self-aligned regrowth of a heavily doped extrinsic base on a moderately doped intrinsic base is studied as a path to higher  $f_{max}$  operation. A thick and heavily carbon doped regrown GaAs ( $4\times 10^{20}\text{cm}^{-3}$ ) extrinsic base provides ample room for metal contact sinking and low  $\rho_c$ , while an InGaAs intrinsic base ( $7\times 10^{19}\text{cm}^{-3}$ ) maintains moderate  $\beta$  for reasonable NF.

The intrinsic HBT epitaxy in this work is similar to that in [4]. A  $520\text{nm}$  refractory Mo/Ti<sub>4wt%</sub>W emitter metal contact is co-sputtered and dry etched in SF<sub>6</sub>/Ar to form  $<100\text{nm}$   $W_e$ . A  $15\text{nm}$  thick PECVD SiN sidewall is deposited. To reveal the intrinsic InGaAs base, the InP emitter is wet etched in 1:4 HCl:H<sub>3</sub>PO<sub>4</sub>. Samples are loaded immediately into a Thomas Swan horizontal flow MOCVD reactor. Surface oxide desorption is carried out at  $540^\circ\text{C}$  for 3min in H<sub>2</sub> with group-V overpressure provided by tertiarybutylphosphine (TBP) to protect the InP emitter sidewall surface. Trimethylgallium (TMGa), tertiarybutylarsine (TBAs), and carbon tetrabromide (CBr<sub>4</sub>) are employed to grow  $\sim 50\text{nm}$  heavily doped GaAs ( $4\times 10^{20}\text{cm}^{-3}$ ). The samples are subject to an in-situ N<sub>2</sub> anneal at  $475^\circ\text{C}$  for 3min before cooldown to drive out hydrogen passivation of  $p$ -type dopants. Base contact metal, Pt/Ru/Pd/Au 5/11/16.5/100nm, is then deposited. Subsequent base/collector mesa isolation, collector metal contact, and device backend processes (Fig. 1-2) are similar to that in [4], except that the base/collector mesa includes a large base metal contact pad area ( $35\times 35\mu\text{m}^2$ ) for direct DC probing. This enables fast DC device turnaround.

Fig. 3 shows measured HBT characteristics of RG67D.  $W_e=100\text{nm}$  devices exhibit a peak current gain  $\beta\sim 15$ , and a common-emitter breakdown voltage  $BV_{CEO}=3.6\text{V}$  ( $J_C=10\mu\text{A}/\mu\text{m}^2$ ). Measurement of the  $1/\beta$  versus  $1/W_e$  relationship indicates that periphery recombination limits device current gain. Base current ideality is  $\sim 4$  for  $0.4\text{V}<V_{BE}<1\text{V}$ , suggesting a large deep defect level recombination current [5]. Since base current does not have a strong dependency on  $V_{CB}$ , it is suspected that the recombination current originates at the  $p^+-p$  extrinsic/intrinsic base interface. Collector current ideality  $\sim 1.3$  is similar to that in [4] with similar intrinsic epi design. Total emitter access resistivity  $\rho_{ex}\sim 4.5\Omega\text{-}\mu\text{m}^2$  is measured by the emitter flyback method. RG67A, a different sample, processed similarly but without the in-situ  $475^\circ\text{C}$  N<sub>2</sub> anneal in MOCVD shows  $\rho_{ex}\sim 3.7\Omega\text{-}\mu\text{m}^2$ . The discrepancy in  $\rho_{ex}$  suggests degradation of the Mo/Ti<sub>4wt%</sub>W emitter metal contact in N<sub>2</sub>. On-wafer transmission line measurement (TLM) results in Fig. 4 show a contact resistivity  $\rho_{bc,ex}=0.4\Omega\text{-}\mu\text{m}^2$  between the base metal contact and GaAs extrinsic base, and an overall contact resistivity  $\rho_{bc,tot}=1.0\Omega\text{-}\mu\text{m}^2$  between the GaAs/metal composite base contact and InGaAs intrinsic base. The sheet resistance of the intrinsic InGaAs base is larger for wider emitters than it is for narrow emitters, corresponding to hydrogen passivation below the InP emitter being harder to reverse [6]. For  $W_e<300\text{nm}$ , however, an intrinsic base sheet resistance  $\rho_{b,sh}=1940\Omega/\text{sq}$ . appears constant.

In this work, we demonstrate an InP/InGaAs DHBT technology with a MOCVD regrown GaAs extrinsic base self-aligned to  $W_e=100\text{nm}$  InP emitter for low base resistance  $R_{bb}$ , and high DC current gain  $\beta$ . Low  $R_{bb}$  is necessary for  $>2\text{THz}$   $f_{max}$  operation, while high  $\beta$  enhances device NF. DC device results show the survival of the refractory Mo/Ti<sub>4wt%</sub>W emitter metal contact, and low base contact resistivities with heavily  $p$ -doped GaAs ( $4\times 10^{20}\text{cm}^{-3}$ ) and use of Pt/Ru/Pd/Au base contact metal. This work was supported by the Semiconductor Research Corporation (SRC) and DARPA under the JUMP ComSenTer program.

- [1] M. Rodwell, *et al*, Proc. of IEEE, vol. 96, no.12 (2008) [2] J. Rode, *et al*, IEEE TED, vol 62, p. 2779 (2015)  
[3] M. Urteaga, *et al*, DRC, Santa Barbara, CA (2011) [4] V. Jain, *et al*, DRC, Santa Barbara, CA (2011)  
[5] A. Schenk, *et al*, J. Appl. Phys., 78, 3185 (1995) [6] S. Stockman, *et al*, J. Electron. Mater., 21:1111 (1992)

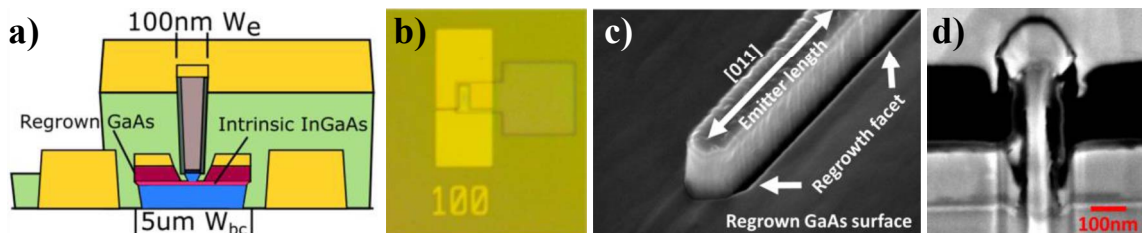


**Fig. 1.** DC device cross-sectional schematic of an 100nm  $W_e$  device with large base/collector mesa for fast turnaround (a); Top view of a  $W_e=100\text{nm}$  device before M1 deposition (b); Tilted SEM view of the regrown GaAs surface (c); SEM of 100nm  $W_e$  device (d)

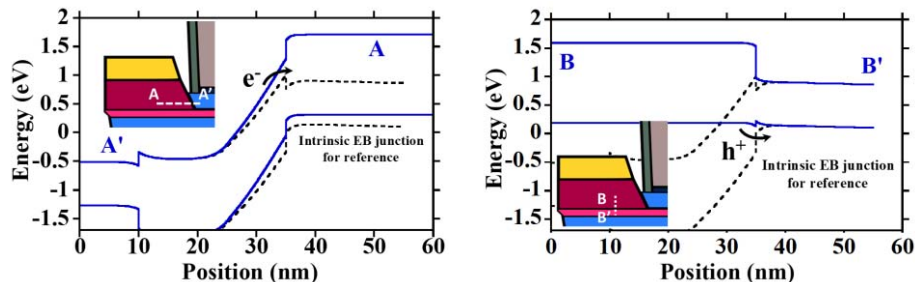


**Fig. 2.** The larger bandgap of regrown GaAs vs. InGaAs prevents electron injection from the emitter to the extrinsic base (left); heavy GaAs doping ( $4 \times 10^{20} \text{cm}^{-3}$ ) minimizes the InGaAs/GaAs valence-band barrier.

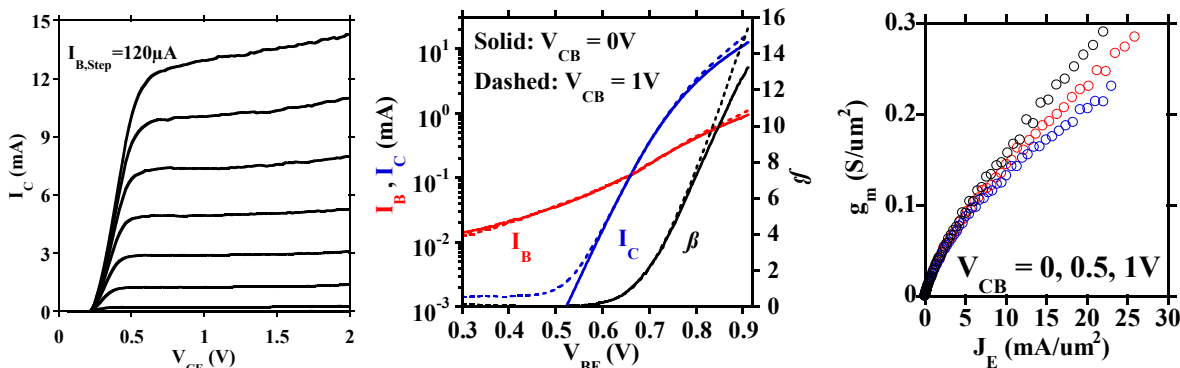


**Fig. 3.** Output, Gummel, and transconductance characteristics of a  $0.09 \times 5 \mu\text{m}^2$  device; the positive output conductance is due to the large base/collector mesa dimensions ( $35 \times 35 \mu\text{m}^2$ )

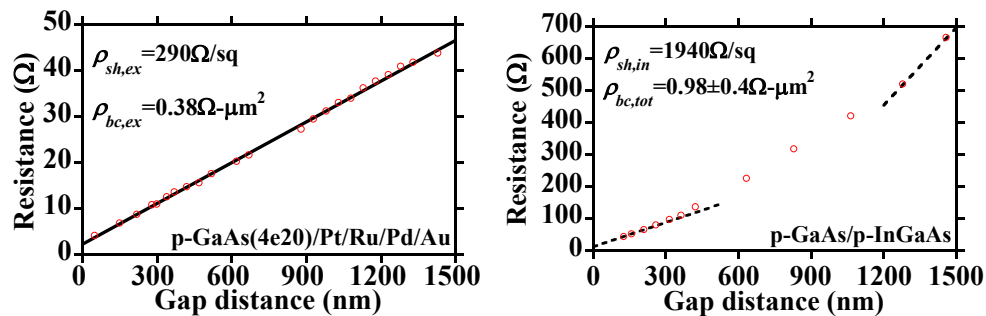


**Fig. 4.** On wafer TLM results showing  $\rho_{sh,ex}$  of regrown extrinsic GaAs, and metal/GaAs contact resistance  $\rho_{bc,ex}$  (left);  $\rho_{sh,in}$  of intrinsic InGaAs, and metal/GaAs/InGaAs contact resistance  $\rho_{bc,tot}$  (right);